DALTON
FULL PAPER

Synthesis of a new tetra-cyanomethylated macrocyclic ligand with a nanotubular structure. X-Ray crystal structures of mono-, di-nuclear and polymeric metal complexes

Sonia González,[a] Laura Valencia,[a] Rufina Bastida,*[a] David E. Fenton,[b] Alejandro Macías[a] and Adolfo Rodríguez[a]

[a] *Departamento de Química Inorgánica, Universidad de Santiago de Compostela, 15782 Santiago de Compostela, Spain. E-mail: qibastid@usc.es*
[b] *Department of Chemistry, The University of Sheffield, Sheffield, UK S3 7HF*

Received 15th May 2002, Accepted 9th July 2002
First published as an Advance Article on the web 23rd August 2002

A new pendant-armed macrocyclic ligand, L^1, bearing four cyanomethyl pendant groups has been synthesized by N-alkylation of the tetraazamacrocyclic precursor L with bromoacetonitrile. The X-ray structural analysis of the ligand L^1 shows the formation of tubular arrays, and reveals intra- and inter-molecular π-stacking interactions between the pyridyl groups of the macrocyclic backbone. Metal complexes of L^1 have been synthesized and characterized by microanalysis, MS-FAB, conductivity measurements, IR, UV-Vis, ^{1}H and ^{13}C NMR spectroscopy and magnetic studies. Crystal structures of the ligand L^1 as well as of the complexes $[ZnL^1](NO_3)_2{\cdot}2H_2O$, $[Ag_2L^1(NO_3)_2]$ and $[Ag_2L^1](ClO_4)_2{\cdot}4CH_3CN$ have been determined by single crystal X-ray crystallography. Different macrocyclic disposition has been found in relation to the metal ion employed and even when different salts of the same metal are used. The X-ray studies show the presence of two metal atoms within the macrocyclic ligand in $[Ag_2L^1(NO_3)_2]$ and $[Ag_2L^1](ClO_4)_2{\cdot}4CH_3CN$ showing a monomeric and a polymeric nature respectively. The crystal structure of $[ZnL^1(NO_3)_2]{\cdot}2H_2O$ shows a mononuclear endomacrocyclic complex with the metal ion coordinated to the six nitrogen atoms in a distorted octahedral environment.

Introduction

Metal-ion coordination by pyridine-containing polyaza macrocycles has been extensively investigated in the last few years.[1] The presence of the pyridine groups in the macrocyclic framework offers the opportunity to obtain highly stable metal complexes and it has been shown to produce molecular helicity in inorganic complexes, which has attracted considerable interest in recent years[2–4] for its importance in nature.

Rothermel *et al.*[5] synthesized and studied the 18-membered hexaazamacrocycle L derived from 2,6-diformylpyridine and ethylenediamine. It has been shown that the role of the metal ion size is essential in controlling the conformation of this type of macrocycle.[6]

Organic tubular assemblies are of interest due to their numerous possible applications, many of which are evident from a consideration of biological systems. Due to numerous potential applications in areas such as chemistry, biology, and materials science considerable effort has recently been devoted to the preparation of artificial nanotubular structures. Macrocyclic ligands bearing cyanoethyl or cyanomethyl pendant groups have been previously synthesized.[7] Schröder *et al.* used mononuclear silver complexes with a macrocyclic ligand to obtain one-dimensional and three-dimensional polymeric compounds. Here, the new macrocycle L^1, having four pendant cyanomethyl groups has been synthesized starting from the macrocycle L (Fig. 1). The X-ray structural analysis of L^1 shows the formation of tubular arrays, and reveals intra- and intermolecular π-stacking interactions between the pyridyl groups of the macrocyclic backbone.

In previous work we have reported the coordination capability of the oxaazamacrocyclic ligands derived from the condensation between 2,6-diformylpyridine and different diamines having two aromatic spacers.[8] In this work the coordination ability of the new pendant-armed macrocyclic ligand L^1 towards different metal ions has been investigated. Due to the linear nature of the nitrile groups it is not possible for intramolecular coordination to their parent metal ion to occur, but intermolecular coordination to other metal ions gives rise to polymeric structures. Metal complexes of L^1 with Cu(II), Co(II), Ni(II), Zn(II), Cd(II), and Ag(I) have been prepared and characterized by microanalysis, MS-FAB, conductivity measurements, IR, UV-Vis, ^{1}H and ^{13}C NMR spectroscopy and magnetic studies. X-Ray diffraction studies on $[ZnL^1](NO_3)_2{\cdot}2H_2O$, $[Ag_2L^1(NO_3)_2]$ and $[Ag_2L^1](ClO_4)_2{\cdot}4CH_3CN$ show the helical shape of the Zn(II) macrocyclic complex, whilst the reaction between silver salts and L^1 give rise to dinuclear endomacrocyclic complexes with monomeric or polymeric arrays.

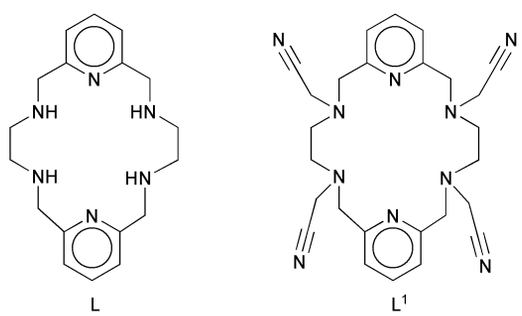

L L^1

Fig. 1

Results and discussion

The cyclocondensation of ethylenediamine and 2,6-pyridine dicarbaldehyde, in the presence of Ca^{2+} as a templating agent followed by an *in situ* demetallation reaction to yield the

Table 1 ^{1}H NMR (δ/ppm) spectra for L^1, $[ZnL^1](ClO_4)_2$, $[Ag_2L^1(NO_3)_2]$ and $[CdL^1](NO_3)_2$ in DMSO-d_6

Assignment	L^1	$[ZnL^1](ClO_4)_2$	$[Ag_2L^1(NO_3)_2]$	$[CdL^1](NO_3)_2$
Ha	7.69 (t, 2H)	8.34 (t, 2H)	8.01 (t, 2H)	8.27 (t, 2H)
Hb	7.21 (d, 4H)	7.87 (d, 4H)	7.52 (d, 4H)	7.79 (d, 4H)
Hc_1 and Hc_2	3.87 (s, 8H)	4.40 (d, 4H), 4.28 (d, 4H)	3.87 (s, 8H)	4.28 (br, 8H)
Hd_1 and Hd_2	2.57 (s, 8H)	2.82 (d, 4H), 2.70 (d, 4H)	2.82 (s, 8H)	2.99 2.85 (br, 8H)
He_1 and He_2	3.59 (s, 8H)	4.12 (d, 4H), 3.93 (d, 4H)	3.72 (s, 8H)	4.15 (br, 8H)

Table 2 ^{1}H NMR (δ/ppm) spectra for L^1, $[ZnL^1](NO_3)_2$ and $[Ag_2L^1](ClO_4)_2\cdot 4CH_3CN$ in CD_3CN

Assignment	L^1	$[ZnL^1](NO_3)_2$	$[Ag_2L^1](ClO_4)_2\cdot 4CH_3CN$
Ha	7.76 (t, 2H)	8.42 (t, 2H)	8.04 (t, 2H)
Hb	7.32 (d, 4H)	7.86 (d, 4H)	7.55 (d, 4H)
Hc_1 and Hc_2	3.88 (s, 8H)	4.54 (d, 4H), 4.35 (d, 4H)	3.97 (s, 8H)
Hd_1 and Hd_2	2.78 (s, 8H)	2.79 (d, 4H), 3.04 (br)	2.98 (s, 8H)
He_1 and He_2	3.77 (s, 8H)	3.94 (d, 4H), 3.76 (d, 4H)	3.61 (s, 8H)

tetraamine ligand L, is reported elsewhere.[5,9,10] The tetracyanomethylated ligand L^1 was obtained through the N-alkylation of the secondary aromatic amines present in the ligand L in acetonitrile using bromoacetonitrile as alkylating agent with Na_2CO_3 as base. Under these conditions the alkylation reaction proceeds readily to give exclusively the tetraalkylated compound. The product was isolated as an air-stable pale yellow solid in 56% yield and was characterized by elemental analysis, FAB MS, IR, ^{1}H and ^{13}C NMR spectroscopy and X-ray diffraction.

The infrared spectrum (KBr disc) of the macrocycle shows $\nu_{(C=N)}$ and $\nu_{(C=C)}$ vibrations from the pyridine groups at 1594 and 1457 cm^{-1}. The disappearance of the secondary amine stretch in the IR spectrum of L^1 is observed, confirming that the alkylation reaction took place (this band appears at 3297 cm^{-1} in the precursor ligand L). The $\nu_{(C\equiv N)}$ band from the pendant groups appears as a weak band at 2225 cm^{-1}.[11] The FAB mass spectrum shows the parent peak at *m*/*z* 483 further confirming the presence of the tetracyanomethylated macrocyclic ligand L^1.

The ^{1}H (Tables 1 and 2) and ^{13}C NMR spectra of L^1 were recorded in deuterated acetonitrile and dimethyl sulfoxide, and confirm the integrity of the ligand and their stability in solution. The spectra show that the four quadrants of the macrocyclic ligand are chemically equivalent as is usual in this kind of ligand. The pyridine hydrogens Ha and Hb exhibit the expected triplet and doublet splitting patterns and chemical shifts, and three singlet signals appears in the aliphatic region of the spectra corresponding to Hc, Hd and He.

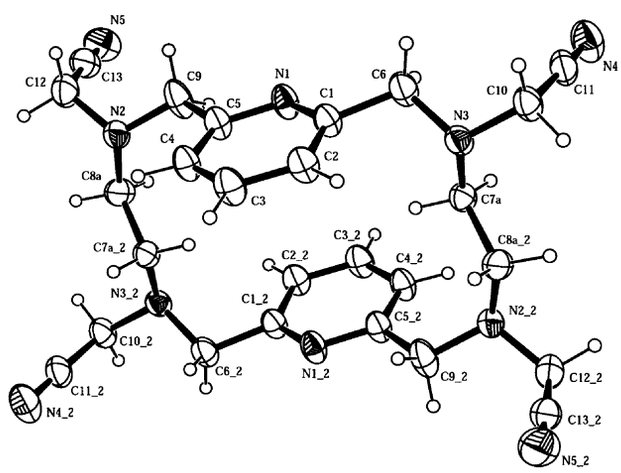

Fig. 2 Crystal structure for L^1.

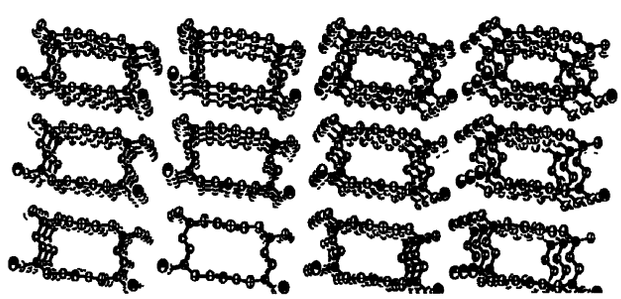

Fig. 3 Disposition of the ligand in the crystal cell.

Crystal structure of L^1

The molecular structure for L^1 is given in Fig. 2, and belongs to the triclinic space group $P\bar{1}$ with the crystallographic inversion centre located in the macrocyclic cavity. The carbon atoms of the ethylene bridges are disordered over two positions with occupancy factors of 0.79 for C7a and C8a and 0.21 for C7b and C8b (the disorder is omitted in the figure for simplicity).

The bond lengths and angles in the structure all fall within the normal ranges. The two pyridine rings are forced to be coplanar for symmetry and the four aliphatic nitrogen atoms of the macrocyclic backbone are also in a plane. The molecule has a markedly stepped conformation, with a dihedral angle of 77.30° between the plane containing the pyridyl groups and the plane that contains the four aliphatic nitrogen atoms.

The X-ray structural analysis of L^1 shows the formation of hollow tubular structures of molecular dimensions called nanotubes (Fig. 3). In the preparation of such tubular assemblies, biological systems make extensive use of self-assembling and self-organizing strategies. In this case, the crystal structure reveals intra- and inter-molecular π-stacking interactions between the pyridyl groups of the macrocyclic ligand. The intramolecular distance between the centroids of the pyridyl rings is 4.75 Å and the intramolecular distance between the centroids of contiguous pyridyl rings is 4.42 Å.

The macrocycle shows the pendant groups attached to contiguous nitrogen atoms lying on opposites sides of the ring.

Metal complexes of L^1

Complexation reactions between the ligand L^1 with hydrated metal salts were carried out in order to investigate the coordination capability of the ligand. All the complexes were prepared by reaction of L^1 with the appropriate metal salt in acetonitrile. Analytical data were in accord with the formation of mononuclear complexes of the type $[ML^1]X_2$ where M = Cu^{2+}, Ni^{2+}, Co^{2+}, Zn^{2+} or Cd^{2+} and X = NO_3^- or ClO_4^-. The

use of hydrated silver salts gave rise to the dinuclear compounds $[Ag_2L^1(NO_3)_2]$ and $[Ag_2L^1](ClO_4)_2{\cdot}4CH_3CN$.

The molar conductivities of the complexes in DMF fall within the range reported for 2 : 1 electrolytes in this solvent.[12]

The IR spectra of the complexes were recorded using KBr discs and all show similar features. The $\nu_{C\equiv N}$ of the pyridine groups are shifted to higher wavenumber than in the free ligand suggesting coordination of the pyridine groups to the metal atom.[13] The $\nu_{C\equiv N}$ band of the pendant groups is not observed in the IR spectra of most of the complexes, although it appears in the free ligand as a weak band at 2225 cm^{-1}. A weak band at 2264 cm^{-1} appears in the IR spectrum of $[Ag_2L^1](ClO_4)_2{\cdot}4CH_3CN$, being slightly shifted in comparison to its position in the spectrum of the free ligand. This could be indicative of coordination of the ligand to a metal ion although it could also be assigned to the $\nu_{C\equiv N}$ band from the acetonitrile molecules that are coordinated to the silver atoms.

The IR spectra of the perchlorate complexes feature absorptions attributable to ionic perchlorate at *ca.* 1100 cm^{-1}. The lack of splitting of this band indicates that there is no coordination of these groups to the metal centers.[14,15] As found for the perchlorate complexes the vibrations associated with the nitrate groups suggest the presence of ionic nitrates for all the complexes except for the dinuclear silver complex $[Ag_2L^1(NO_3)_2]$ which shows the presence of several bands in the region associated with nitrate vibrations that clearly identifies this complex as containing coordinated nitrate groups.[16] The two most intense nitrate absorptions, associated with the $\nu_{(N=O)}$ and $\nu_{a(NO_2)}$ appear at 1466 and 1301 cm^{-1} respectively, suggesting the presence of bidentate nitrate groups for the silver complex.[17]

Positive-ion FAB mass spectrometry provides key evidence for the formation of some of the complexes. For $[CoL^1](NO_3)_2$, $[CdL^1](NO_3)_2$ and $[ZnL^1](NO_3)_2$ the highest-mass peak in each case corresponds to the general formulation $[ML^1X]^+$ and the loss of a second counterion occurs to generate $[ML^1]^+$. For $[NiL^1](ClO_4)_2$ and $[Ag_2L^1](ClO_4)_2{\cdot}4CH_3CN$ only a peak attributable to $[NiL^1]^+$ and $[AgL^1]^+$ was observed. Due to the low solubility of most of these complexes in the matrix used no peaks could be assigned to any fragmentation for the other complexes.

The ^1H NMR spectra of the diamagnetic complexes $[ZnL^1](ClO_4)_2$, $[Ag_2L^1(NO_3)_2]$ and $[CdL^1](NO_3)_2$ recorded in DMSO-d_6, and $[ZnL^1](NO_3)_2$ and $[Ag_2L^1](ClO_4)_2{\cdot}4CH_3CN$ recorded in CD_3CN, are listed in Tables 1 and 2 respectively, with representative spectra shown in Figs. 4 and 5. The assignments for the spectra correspond to the labeling shown in Fig. 6. As in the free ligand the four quadrants of the macrocyclic ligand are chemically equivalent, and only one pattern is observed for each of Ha, Hb, Hc_1, Hc_2, Hd_1, Hd_2, He_1 and He_2.

The X-ray crystal structure of the Zn^{2+} complex, shows that the stereochemistry at the amine nitrogen sites corresponds to *RRRR* or *SSSS* chirality when coordinated, and this is the only one isomer for L^1 having three C_2 rotational axes and capable of twisting to make a meridional pseudooctahedral complex with D_2 symmetry, to give the chemically equivalent four quadrants of the macrocyclic ligand in the complex. In the ^1H NMR spectrum of $[ZnL^1](ClO_4)_2$ the pyridine hydrogens Ha and Hb exhibit the expected triplet and doublet splitting patterns and chemical shifts. The geminal protons Hc_1 and Hc_2, Hd_1 and Hd_2, He_1 and He_2 appear to separate into doublets showing that they are chemically and magnetically non-equivalent, and the Δλλ (Δδδ) enantiomeric forms are not rapidly interconverted in solution on the time scale of the NMR experiment.

The assignments of the proton signals were based upon standard 2D homonuclear (COSY) and $^1H/^{13}C$ heteronuclear spectra (HMQC). The HMQC spectrum confirms the connectivities between Hc_1/Hc_2 and C_4, Hd_1/Hd_2 and C_5 and He_1/He_2 and C_6, and the COSY spectrum verifies that each of these protons are coupled to their corresponding geminal proton

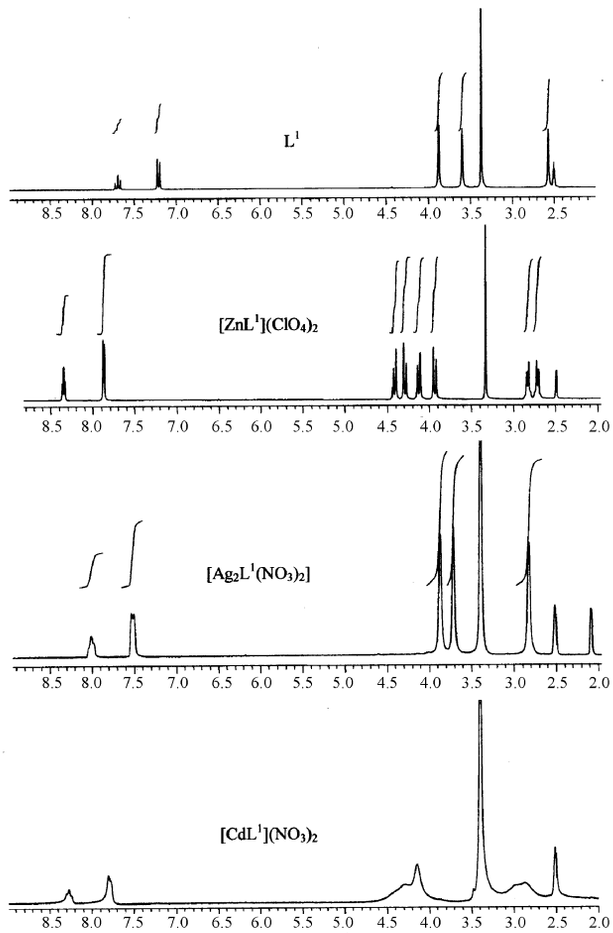

Fig. 4 ^1H NMR spectra for L^1, $[ZnL^1](ClO_4)_2$, $[Ag_2L^1(NO_3)_2]$ and $[CdL^1](NO_3)_2$ in DMSO-d_6.

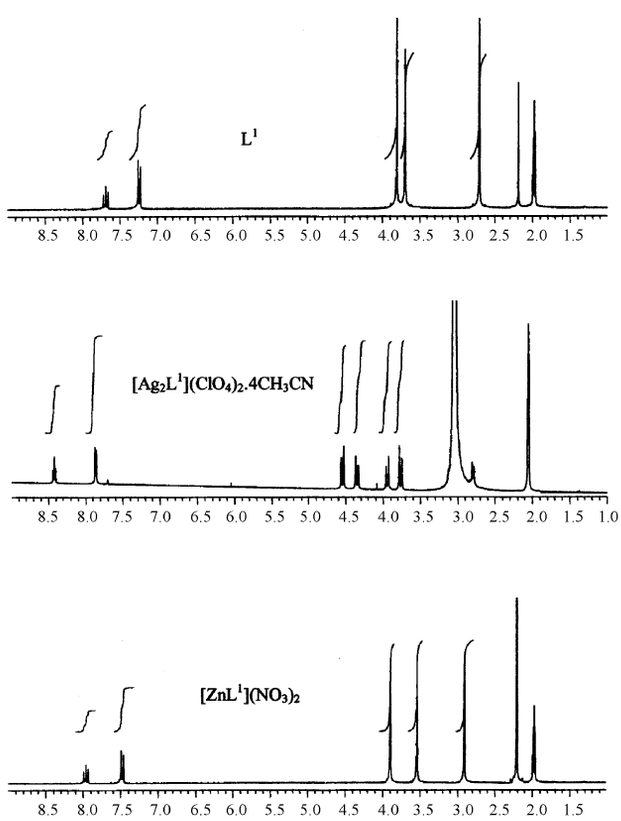

Fig. 5 ^1H NMR spectra for L^1, $[Ag_2L^1](ClO_4)_2{\cdot}4CH_3CN$ and $[ZnL^1](NO_3)_2$ in CD_3CN.

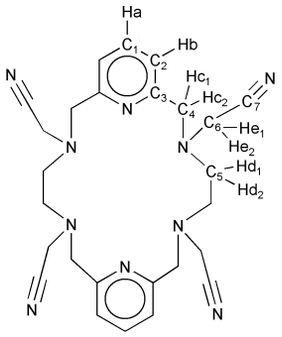

Fig. 6 Labeling scheme for L^1.

with coupling constants $J_{Hc1/Hc2}$ 16.6 Hz; $J_{He1/He2}$ 11.7 Hz and $J_{Hd1/Hd2}$ 17.2 Hz.

The ^{1}H NMR spectrum for $[CdL^1](NO_3)_2$ was recorded in DMSO-d_6. The chemical shifts for the pyridine hydrogens are similar to those for the $[ZnL^1](ClO_4)_2$ complex in DMSO-d_6. The spectrum shows a broad overlapping resonance for Hc_1/Hc_2, Hd_1/Hd_2 and He_1/He_2 showing that a rapid conformational interconversion takes place in solution at this temperature, and it may be related to the larger size of Cd^{2+}, which, as it has been previously seen, causes the macrocycle to twist down less tightly and thus leads to a lower energy barrier for conformational interconversion.[18] The low solubility of the $[CdL^1](NO_3)_2$ complex in solvents other than DMSO prevented us recording the low temperature spectrum. The ^{1}H NMR spectrum for $[ZnL^1](NO_3)_2$ has been recorded in CD_3CN, and as in $[ZnL^1](ClO_4)_2$, Hc_1/Hc_2, Hd_1/Hd_2 and He_1/He_2 separate into doublets showing that they are chemically and magnetically non-equivalent. As expected, the geminal coupling constants between Hc_1/Hc_2, Hd_1/Hd_2 and He_1/He_2 are exactly the same as for $[ZnL^1](ClO_4)_2$ showing that the presence of the nitrate groups does not affect the conformation of the cationic complex in solution.

The ^{1}H NMR spectra of $[Ag_2L^1(NO_3)_2]$ and $[Ag_2L^1](ClO_4)_2\cdot 4CH_3CN$ have been recorded in DMSO-d_6, and CD_3CN respectively. The pyridinic hydrogens Ha and Hb appear again as a triplet and a doublet respectively. As in the Cd^{2+} complex they show an overlapping resonance for Hc_1/Hc_2, Hd_1/Hd_2 and He_1/He_2. In these cases, the rapid conformational interconversion between both isomers is easier in solution at room temperature due to the helix unravelling to form approximately a planar array around the metal ions, as it has been seen in the X-ray crystal structure of $[Ag_2L^1(NO_3)_2]$ and $[Ag_2L^1](ClO_4)_2\cdot 4CH_3CN$.

The solid state electronic spectra of $[CoL^1](ClO_4)_2$, $[CoL^1](NO_3)_2$, $[NiL^1](ClO_4)_2$, $[NiL^1](NO_3)_2$ and $[CoL^1](ClO_4)_2$ show a distorted octahedral environment for all the complexes. The Co(II) complexes show two d–d transition bands at *ca.* 590 and 923 nm attributable to the $^4T_{1g}(F) \longrightarrow {}^4T_{1g}(P)$ and $^4T_{1g}(F) \longrightarrow {}^4T_{2g}(F)$ transitions, that are of the type expected for distorted octahedral Co(II) complexes. The Ni(II) complexes show three bands at *ca.* 320, 550 and 920 nm, attributable to the $^3A_{2g} \longrightarrow {}^3T_{1g}(P)$, $^3A_{2g} \longrightarrow {}^3T_{1g}(F)$ and $^3A_{2g} \longrightarrow {}^3T_{2g}(F)$ transitions respectively, characteristic of Ni(II) complexes in an octahedral environment.[19] The Cu(II) complex shows a broad band with a maximum at *ca.* 705 nm and a shoulder at 1360 nm suggesting a distorted octahedral environment.[20]

The value of the room temperature magnetic moments of $[CoL^1](ClO_4)_2$, (4.8 μ_B) $[CoL^1](NO_3)_2$ (5.0 μ_B), $[NiL^1](ClO_4)_2$ (2.8 μ_B), $[NiL^1](NO_3)_2$ (2.9 μ_B) and $[CuL^1](ClO_4)_2$ (1.8 μ_B) complexes lies within the range usually observed for high-spin octahedral Co(II), Ni(II) and Cu(II) complexes.[21]

Crystal structure of $[ZnL^1](NO_3)_2\cdot 2H_2O$

Recrystallisation of $[ZnL^1](NO_3)_2$ from water gave colourless monoclinic crystals containing water molecules as lattice solvent. The molecular structure and selected bond lengths and angles of $[ZnL^1](NO_3)_2\cdot 2H_2O$ are given in Fig. 7, and the crystallographic data is summarised in Table 3. The X-ray crystal structure confirms the presence of a mononuclear endomacrocyclic complex. The metal atom is six coordinated with a distorted octahedral geometry arising from coordination by the six donor nitrogen atoms of the macrocyclic backbone. The crystal structure is centrosymmetric, and both enantiomers (*SSSS*/*RRRR*) are present in the crystal. The pyridinic nitrogen atoms occupy the axial positions of the octahedron, and the four aliphatic amines form the equatorial plane. The coordination sphere is distorted; in that way, N2 and N2_2 are displaced 0.5323 Å above and below the best plane defined by the metal and the four amine nitrogen atoms, and N3 and N3_2 are displaced 0.5363 Å above and below too. The donor atoms of the pendant arm groups are not coordinated to the central ion and they radiate out away from the metal. The pyridinic nitrogen atoms provide the strongest bond to the ion (N1–Zn 2.0603 Å). The bond distances Zn–N2 are equivalents by symmetry at 2.2706(15) Å, and the Zn–N3 bond distances are equivalents too at 2.2671(16) Å. The Zn–N_{py} distances are slightly shorter than in the related $[ZnL](CF_3SO_3)_2$ complex (Zn–N_{py} 2.112(5) Å), but bigger than the Zn–N_{am} distances (2.210(4) Å).[4] The structure shows a 'twist–wrap' conformation, where the macrocyclic ligand wraps round the metal ion by a twisting of the pyridyl bridgehead units relative to each other. The macrocycle adopts a helical shape, with the two pyridine rings oriented at 76.99° relative to each other. For $[ZnL](CF_3SO_3)_2$ the two pyridine rings are oriented 104.5° relative to each other[4] and 91.5° for $[CdL](CF_3SO_3)_2$.[18] The angle of 180° between the coordinated pyridine nitrogen atoms and the metal ion, due to crystallographic symmetry requirements, show that the macrocycle is not folded. The nitrate ions are not coordinated to the metal, and they were refined with no disorder, giving bond distances and angles typical for this ion.

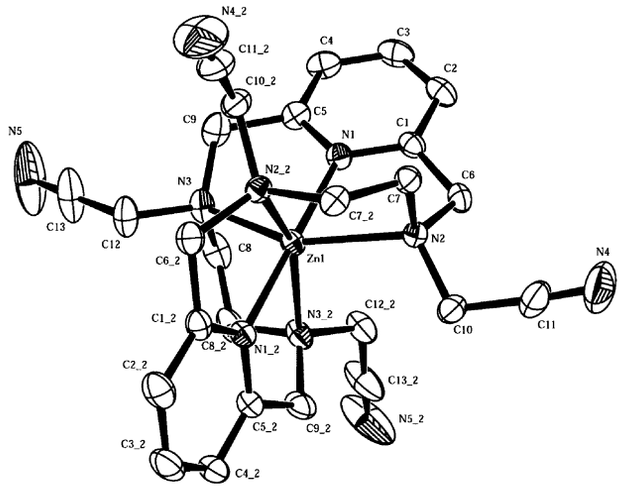

Fig. 7 Crystal structure and selected bond lengths (Å) and angles (°) for $[ZnL^1](NO_3)_2\cdot 2H_2O$. Zn(1)–N(1) 2.0603(15), Zn(1)–N(3) 2.2671(16), Zn(1)–N(2) 2.2706(15); N(1)–Zn(1)–N(1)#1 179.59(8), N(1)–Zn(1)–N(3) 76.44(6), N(1)#1–Zn(1)–N(3) 103.24(6), N(3)–Zn(1) N(3)#1 82.31(9), N(1)–Zn(1)–N(2) 76.32(6), N(3)–Zn(1)–N(2) 152.76(6), N(1)–Zn(1)–N(2)#1 104.00(6), N(3)–Zn(1)–N(2)#1 103.96(6). Symmetry transformations used to generate equivalent atoms: #1 $-x$, y, $-z + 1/2$.

Crystal structure of $[Ag_2L^1(NO_3)_2]$

Recrystallisation of the silver nitrate complex from dimethyl sulfoxide gave colourless monoclinic crystals of $[Ag_2L^1(NO_3)_2]$. The molecular structure and selected bond lengths and angles of $[Ag_2L^1(NO_3)_2]$ are given in Fig. 8 and the crystallographic

Table 3 Crystal data and structure refinement for L^1, $[ZnL^1](NO_3)_2\cdot 2H_2O$, $[Ag_2L^1(NO_3)_2]$ and $[Ag_2L^1](ClO_4)_2\cdot 4CH_3CN$

	L^1	$[ZnL^1](NO_3)_2\cdot 2H_2O$	$[Ag_2L^1(NO_3)_2]$	$[Ag_2L^1](ClO_4)_2\cdot 4CH_3CN$
Empirical formula	$C_{13}H_{15}N_5$	$C_{26}H_{34}N_{12}O_8Zn$	$C_{26}H_{30}N_{12}O_6Ag_2$	$C_{34}H_{42}N_{14}O_8Cl_2Ag_2$
Formula weight	241.30	708.02	822.36	1061.46
Temperature/K	293(2)	293(2)	293(2)	293(2)
Wavelength/Å	1.54180	0.71073	0.71073	0.71073
Crystal system	Triclinic	Monoclinic	Monoclinic	Monoclinic
Space group	$P\bar{1}$	$C2/c$	$P21/n$	$P21/c$
a/Å	6.1800(3)	15.486(3)	9.439(4)	11.423(4)
b/Å	8.3150(3)	12.804(3)	9.229(4)	18.521(7)
c/Å	13.2140(9)	16.421(4)	17.967(9)	11.133(4)
α/°	86.256(4)	—	—	—
β/°	78.343(5)	106.097(4)	104.414(7)	112.304(6)
γ/°	80.581(4)	—	—	—
Volume/Å^3	655.69(6)	3128.4(12)	1516.0(12)	2179.2(14)
Z	2	4	2	2
Absorption coefficient/mm^{-1}	0.623	0.854	1.355	1.086
F(000)	256	1472	824	1072
Crystal size/mm^3	0.48 × 0.36 × 0.20	0.49 × 0.25 × 0.24	0.13 × 0.12 × 0.10	0.55 × 0.22 × 0.17
Reflections collected	2875	9159	11688	11781
Independent reflections	2617 [R(int) = 0.0238]	3214 [R(int) = 0.0193]	3109 [R(int) = 0.0573]	4420 [R(int) = 0.0238]
Absorption correction	Psi-scan	Empirical	Empirical	Empirical
Refinement method	Full-matrix least-squares on F^2	Full-matrix least-squares on F^2	Full-matrix least-squares on F^2	Full-matrix least-squares on F^2
Data/restraints/parameters	2617/0/183	3214/0/213	3109/0/208	4420/0/273
Final R indices [$I > 2\sigma(I)$]	$R1$ = 0.0470, $wR2$ = 0.1364	$R1$ = 0.0315, $wR2$ = 0.0829	$R1$ = 0.0408, $wR2$ = 0.1038	$R1$ = 0.0276, $wR2$ = 0.0646
R indices (all data)	$R1$ = 0.0547, $wR2$ = 0.1437	$R1$ = 0.0391, $wR2$ = 0.0869	$R1$ = 0.0619, $wR2$ = 0.1181	$R1$ = 0.0394, $wR2$ = 0.0702

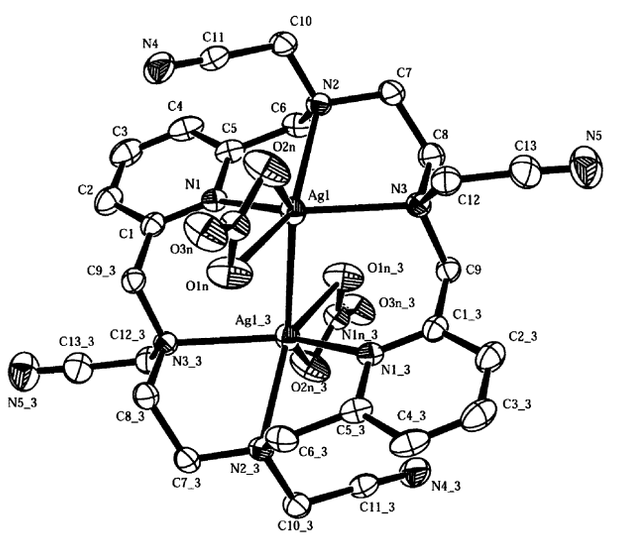

Fig. 8 Crystal structure and selected bond lengths (Å) and angles (°) for $[Ag_2L^1(NO_3)_2]$. Ag(1)–N(1) 2.363(4), Ag(1)–N(3) 2.444(4), Ag(1)–N(2) 2.480(4), Ag(1)–O(1N) 2.496(5), Ag(1)–O(2N) 2.527(4), Ag(1)–Ag(1)#1 2.8476(14); N(1)–Ag(1)–N(3) 129.90(14), N(1)–Ag(1)–N(2) 73.92(13), N(3)–Ag(1)–N(2) 74.55(13), N(1)–Ag(1)–O(1N) 106.34(15), N(3)–Ag(1)–O(1N) 121.07(16), N(2)–Ag(1)–O(1N) 147.31(13), N(1)–Ag(1)–O(2N) 121.96(16), N(3)–Ag(1)–O(2N) 101.79(15), N(2)–Ag(1)–O(2N) 101.52(14), O(1N)–Ag(1)–O(2N) 49.61(13). Symmetry transformations used to generate equivalent atoms: #1 $-x + 2, -y, -z + 2$.

details are summarised in Table 3. The crystal structure is centrosymmetric, and both enantiomers (*SRSR*/*RSRS*) are present in the crystal. The X-ray crystal structure shows the presence of two metal ions in the cavity of the hexaaza macrocyclic ligand giving rise to a dinuclear endomacrocyclic complex. The two silver atoms are equivalent by symmetry, and they are both in identical distorted pentagonal bipyramidal environments coordinated to one pyridinic nitrogen, two secondary amine nitrogen atoms and two oxygen atoms from an asymmetric bidentate nitrate (Ag(1)–O(1N), 2.496(5); Ag(1)–O(2N), 2.527(4) Å). Again the pyridinic nitrogen atoms provide the strongest bond to the silver atoms (N(1)–Ag(1) 2.363(4) Å). The bond distances Ag(1)–N(2) and Ag(1)–N(3) are 2.480(4) and 2.444(4) Å respectively. The distance between the metal centers is 2.8476(14) Å showing interaction between them. The pendant arm groups are not coordinated to the metals.

The macrocyclic ligand is not folded or twisted. The disposition of the macrocycle is quite plane, with a dihedral angle between the pyridyl groups of 0° due to crystallographic symmetry requirements. The best plane defined by the six nitrogen atoms of the ligand backbone has a rms of 0.1039, the silver atoms being situated 0.8311 Å above and below this plane.

Crystal structure of $[Ag_2L^1](ClO_4)_2\cdot 4CH_3CN$

Recrystallisation of the perchlorate silver complex from acetonitrile gave colourless monoclinic crystals of $[Ag_2L^1](ClO_4)_2\cdot 4CH_3CN$. The molecular structure and selected bond lengths and angles are given in Fig. 9 and the crystallographic details are summarised in Table 3.

The crystal structure of the silver complex shows the presence of two metal atoms within the macrocyclic ligand and it also shows the polymeric nature of this compound, with the nitrogen donor atoms of the pendant groups intermolecularly coordinated to the silver atoms. Similar polymeric structures were found by Schröder *at al.*[7] with two tetraazamacrocyclic ligands having three cyanomethyl (L^A) or cyanoethyl (L^B) pendant groups. For L^A, a three-dimensional polymer has been obtained with $AgPF_6$, where each Ag^I ion is coordinated to six N donor atoms (three from the triazamacrocycle and three from the nitrile groups belonging to three different molecules. For L^B a one-dimensional zig-zag silver polymer was obtained with the Ag^I ion in a distorted tetrahedral environment.

As in $[Ag_2L^1(NO_3)_2]$ the two silver atoms are equivalents by symmetry, and they are both in identical distorted pentagonal bipyramidal environments coordinated to one pyridinic nitrogen and two secondary amine nitrogen atoms from the macrocyclic backbone. The coordination number is completed by the coordination to a nitrogen atom from one pendant group from the other macrocyclic unit and by the coordination to a nitrogen atom from an acetonitrile molecule, giving rise to a bidimensional polymeric structure (Fig. 10).

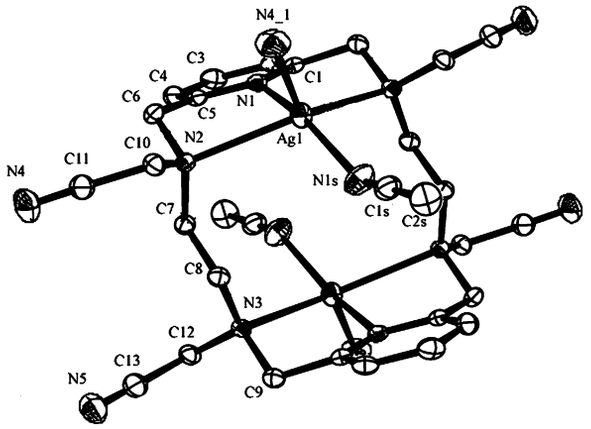

Fig. 9 Crystal structure and selected bond lengths (Å) and angles (°) for $[Ag_2L^1](ClO_4)_2{\cdot}4CH_3CN$. Ag(1)–N(1) 2.278(2), Ag(1)–N(1S) 2.248(3), Ag(1)–N(2) 2.569(2), Ag(1)–N(3)#1 2.624(2), Ag(1)–N(4) 2.348(3); N(1S)–Ag(1)–N(1) 158.56(9), N(1S)–Ag(1)–N(4) 89.95(10), N(1)–Ag(1)–N(4) 111.46(9), N(1S)–Ag(1)–N(2) 106.70(9), N(1)–Ag(1)–N(2) 71.92(7), N(4)–Ag(1)–N(2) 93.79(9), N(1S)–Ag(1)–N(3)#1 99.34(9), N(1)–Ag(1)–N(3)#1 70.91(7), N(4)–Ag(1)–N(3)#1 121.81(8), N(2)–Ag(1)–N(3)#1 135.71(6). Symmetry transformations used to generate equivalent atoms: #1 $-x+1, -y, -z+1$.

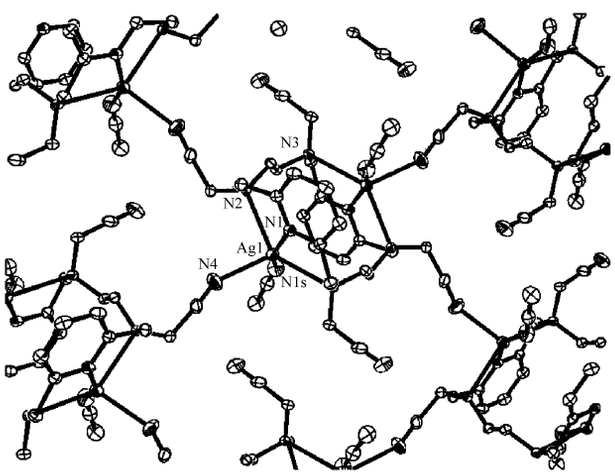

Fig. 10 Polymeric structure for $[Ag_2L^1](ClO_4)_2{\cdot}4CH_3CN$.

In this case, the nitrogen atom from the acetonitrile molecule provides the strongest bond to the silver atoms (N(1S)–Ag(1) 2.248(3) Å), and the distance between the pyridinic nitrogen atom and the metal ion (N(1)–Ag(1) 2.278(2) Å) is shorter than in $[Ag_2L^1(NO_3)_2]$. The bond distances Ag(1)–N(2) and Ag(1)–N(3) are 2.569(2) and 2.624(2) Å respectively. The intermolecular coordination to the silver atoms of one nitrogen atom of the pendant group from another ligand molecule produces the displacement of the metal outside the macrocyclic cavity, and in this case the distance between the metal centers is 4.718 Å.

As in $[Ag_2L^1(NO_3)_2]$ the macrocyclic ligand is not folded or twisted, and the dihedral angle between the pyridyl groups is 0° which is also due to crystallographic symmetry requirements.

In this case the macrocyclic ligand presents a step conformation, similar to the free ligand. The four aliphatic nitrogen atoms of the ligand backbone are in a plane and the silver atoms are sited 0.9347 Å above and below this plane. The dihedral angle between the plane containing the pyridine ring and the plane containing the four aliphatic nitrogen atoms of the ligand backbone is 88.45° showing that they are almost perpendicular to the best plane through the ring of the macrocycle. The distance between centroids in this case is 5.58 Å. The macrocycle shows, as in the free ligand, the pendant groups attached to contiguous nitrogen atoms lying on opposites sides of the ring.

Conclusion

A new ligand, L^1, bearing four cyanomethyl groups has been synthesized. These pendant groups are usually not involved in the coordination of the encapsulated metal, and they could promote the formation of polymeric compounds. The reaction between silver salts and L^1 gave rise to dinuclear endomacrocyclic complexes with monomeric or polymeric arrays. With the nitrate silver salt a dinuclear endomacrocyclic complex $[Ag_2L^1(NO_3)_2]$ was obtained. However, when the perchlorate salt was used the X ray crystal structure showed a polymeric compound with formula $[Ag_2L^1](ClO_4)_2{\cdot}4CH_3CN$. The Zn^{II} complex shows the metal ion endomacrocyclicly coordinated in an octahedral distorted environment.

Experimental

Measurements

Elemental analyses were performed in a Carlo-Erba EA microanalyser. Infrared spectra were recorded as KBr discs on a Bruker IFS-66V spectrophotometer. FAB mass spectra were recorded using a Kratos-MS-50T spectrometer connected to a DS90 data system using 3-nitrobenzyl alcohol as the matrix. Conductivity measurements were carried out in 10^{-3} mol dm^{-3} DMF solutions at 20 °C using a WTW LF3 conductivity meter. ^1H and ^{13}C NMR spectra were recorded on a Bruker AMX 300 MHz instrument against TMS as internal standard and DEPT 135 and HMQC ^1H–^{13}C on a Bruker 500 MHz instrument. Solid state electronic spectra were recorded on a Hitachi 4-3200 spectrophotometer using $MgCO_3$ as reference. Magnetic studies were determined at rt on a vibration sample magnetometer (VSM) Digital Measurement System 1660 with a magnetic field of 5000 G.

Chemicals and starting materials

2,6-Pyridinedimethanol, ethylenediamine, bromoacetonitrile and metal salts were commercial products (from Alfa and Aldrich) and were used without further purification. Solvents were of reagent grade and were purified by the usual methods. **CAUTION!** Perchlorate salts are potentially explosive.

Synthesis of the macrocycle L^1

L (3 mmol, 2 g) was dissolved in acetonitrile (100 mL) under reflux and 2-picolyl chloride hydrochloride (15 mmol, 2.46 g) and Na_2CO_3 (39 mmol, 4.13 g) were added. The mixture was refluxed for 6 hours and then left to cool. The resulting solution was filtered and evaporated to dryness. The residue was then extracted with water–chloroform. The organic layer was dried over $MgSO_4$ and evaporated to yield an orange solid that was recrystallised in acetonitrile giving the ligand L^1 as a pale yellow solid. Found (calc.) for $C_{26}H_{30}N_{10}$ (482.59): C, 64.7 (64.7); H, 6.4 (6.2); N, 28.7 (29.1)%. Yield: 56%. IR (KBr, cm^{-1}): $\nu(C{=}C)_{ar}$ and $\nu(C{=}N)_{py}$ 1594, 1457, $\nu(C{\equiv}N)$ 2225. (FAB, *m*/*z*): $[L^1]^+$ 483. Colour: white.

Synthesis of the metal complexes of L^1

To an acetonitrile solution (20 mL) of L^1 (0.25 mmol, 0.1205 g) was added a solution of the appropriate metal salt (0.3 mmol) in acetonitrile (5 mL) and the solution was heated at reflux for 2 hours. The precipitate began to deposit immediately. The mixture was allowed to cool and the precipitate was subsequently filtered off and dried *in vacuo*. The complexes were found to be air-stable and soluble in dimethyl sulfoxide and

dimethyl formamide, some of them are soluble in water and acetonitrile, and are in general insoluble in absolute ethanol, methanol, diethyl ether, chloroform, dichloromethane and acetone.

$[CuL^1](ClO_4)_2$. Found (calc.) for $C_{26}H_{30}N_{10}Cl_2O_8Cu$ (745.04): C, 41.25 (41.91); H, 4.07 (4.03); N, 18.52 (18.80)%. Yield: 69%. IR (KBr, cm^{-1}): $\nu(C{=}C)_{ar}$ and $\nu(C{=}N)_{py}$ 1610, 1444, [$\nu(ClO_4^-)$] 1092, 625. Λ_M (10^{-3} M, DMF): 158 Ω^{-1} cm^2 mol^{-1} (2 : 1 electrolyte). Colour: blue.

$[NiL^1](ClO_4)_2$. Found (calc.) for $C_{26}H_{30}N_{10}Cl_2O_8Ni$ (740.18): C, 41.78 (42.18); H, 4.07 (4.06); N, 18.67 (18.93)%. Yield: 71%. IR (KBr, cm^{-1}): $\nu(C{=}C)_{ar}$ and $\nu(C{=}N)_{py}$ 1610, 1454, [$\nu(ClO_4^-)$] 1099, 628. MS (FAB, *m*/*z*): $[NiL^1]^+$ 541. Λ_M (10^{-3} M, DMF): 175 Ω^{-1} cm^2 mol^{-1} (2 : 1 electrolyte). Colour: violet.

$[CoL^1](ClO_4)_2$. Found (calc.) for $C_{26}H_{30}N_{10}Cl_2O_8Co$ (740.43): C, 42.28 (42.17); H, 4.05 (4.08); N, 18.34 (18.92)%. Yield: 62%. IR (KBr, cm^{-1}): $\nu(C{=}C)_{ar}$ and $\nu(C{=}N)_{py}$ 1614, 1442, [$\nu(ClO_4^-)$] 1093, 628. Λ_M (10^{-3} M, DMF): 167 Ω^{-1} cm^2 mol^{-1} (2 : 1 electrolyte). Colour: blue.

$[ZnL^1](ClO_4)_2$. Found (calc.) for $C_{26}H_{30}N_{10}Cl_2O_8Zn$ (746.87): C, 41.25 (41.80); H, 4.00 (4.02); N, 18.43 (18.76)%. Yield: 74%. IR (KBr, cm^{-1}): $\nu(C{=}C)_{ar}$ and $\nu(C{=}N)_{py}$ 1610, 1442, [$\nu(ClO_4^-)$] 1093, 628. Λ_M (10^{-3} M, DMF): 183 Ω^{-1} cm^2 mol^{-1} (2 : 1 electrolyte). Colour: white. ^{13}C NMR δ (ppm): C_1, 143.2; C_2, 125.2; C_3, 152.1; C_4, 52.3; C_5, 50.7; C_6, 42.1; C_7, 114.3.

$[Ag_2L^1(ClO_4)_2]\cdot 4CH_3CN$. Found (calc.) for $C_{34}H_{42}N_{14}O_8Cl_2Ag_2$ (1061.44): C, 38.2 (38.5); H, 3.6 (4.0); N, 18.4 (18.5)%. Yield: 52%. IR (KBr, cm^{-1}): $\nu(C{=}C)_{ar}$ and $\nu(C{=}N)_{py}$ 1602, 1450, [$\nu(ClO_4^-)$] 1093, 623. MS (FAB, *m*/*z*): $[AgL^1]^+$ 591. Λ_M (10^{-3} M, DMF): 189 Ω^{-1} cm^2 mol^{-1} (2 : 1 electrolyte). Colour: grey.

$[NiL^1](NO_3)_2$. Found (calc.) for $C_{26}H_{30}N_{12}O_6Ni$ (665.29): C, 46.59 (46.94); H, 4.1 (4.6); N, 25.32 (25.26)%. Yield: 69%. IR (KBr, cm^{-1}): $\nu(C{=}C)_{ar}$ and $\nu(C{=}N)_{py}$ 1619, 1431, [$\nu(NO_3^-)$] 815, 1384. Λ_M (10^{-3} M, DMF): 183 Ω^{-1} cm^2 mol^{-1} (2 : 1 electrolyte). Colour: violet.

$[CoL^1](NO_3)_2$. Found (calc.) for $C_{26}H_{30}N_{12}O_6Co$ (665.53): C, 45.71 (46.92); H, 4.43 (4.51); N, 25.15 (25.27)%. Yield: 76%. IR (KBr, cm^{-1}): $\nu(C{=}C)_{ar}$ and $\nu(C{=}N)_{py}$ 1611, 1429, [$\nu(NO_3^-)$] 813, 1384. MS (FAB, *m*/*z*): $[CoL^1(NO_3)]^+$ 603, $[CoL^1]^+$ 541. Λ_M (10^{-3} M, DMF): 158 Ω^{-1} cm^2 mol^{-1} (2 : 1 electrolyte). Colour: blue.

$[ZnL^1](NO_3)_2$. Found (calc.) for $C_{26}H_{30}N_{12}O_6Zn$ (675.97): C, 45.20 (46.47); H, 4.43 (4.50); N, 24.23 (25.02)%. Yield: 75%. IR (KBr, cm^{-1}): $\nu(C{=}C)_{ar}$ and $\nu(C{=}N)_{py}$ 1610, 1427, [$\nu(NO_3^-)$] 811, 1384. MS (FAB, *m*/*z*): $[ZnL^1(NO_3)]^+$ 608, $[ZnL^1]^+$ 548. Λ_M (10^{-3} M, DMF): 167 Ω^{-1} cm^2 mol^{-1} (2 : 1 electrolyte). Colour: white.

$[CdL^1](NO_3)_2$. Found (calc.) for $C_{26}H_{30}N_{12}O_6Cd$ (719.01): C, 43.20 (43.43); H, 4.33 (4.18); N, 23.71 (23.39)%. Yield: 90%. IR (KBr, cm^{-1}): $\nu(C{=}C)_{ar}$ and $\nu(C{=}N)_{py}$ 1604, 1457, [$\nu(NO_3^-)$] 821, 1384. MS (FAB, *m*/*z*): $[CdL^1(NO_3)]^+$ 657, $[CdL^1]^+$ 595. Λ_M (10^{-3} M, DMF): 150 Ω^{-1} cm^2 mol^{-1} (2 : 1 electrolyte). Colour: white.

$[Ag_2L^1(NO_3)_2]$. Found (calc.) for $C_{26}H_{30}N_{12}O_6Ag_2$ (822.34): C, 37.67 (37.98); H, 3.56 (3.68); N, 19.84 (20.44)%. Yield: 72%. IR (KBr, cm^{-1}): $\nu(C{\equiv}N)$ 2264, $\nu(C{=}C)_{ar}$ and $\nu(C{=}N)_{py}$ 1600, 1452, [$\nu(NO_3^-)$] 815, 1301, 1384, 1466. Λ_M (10^{-3} M, DMF): 167 Ω^{-1} cm^2 mol^{-1} (2 : 1 electrolyte). Colour: grey.

X-Ray crystallography

The crystals were obtained by slow recrystallisation from acetonitrile for L^1 and $[Ag_2L^1](ClO_4)_2\cdot 4CH_3CN$, from water for $[ZnL^1](NO_3)_2\cdot 2H_2O$ and from dimethyl sulfoxide for $[Ag_2L^1(NO_3)_2]$. The details of the X-ray crystal data, and the structure solution and refinement are given in Table 3. Measurements were made on a Bruker SMART CCD area diffractometer with graphite-monochromated Mo-Kα radiation for $[ZnL^1](NO_3)_2\cdot 2H_2O$, $[Ag_2L^1(NO_3)_2]$ and $[Ag_2L^1](ClO_4)_2\cdot 4CH_3CN$ and on a MACH3 Enraf Nonius with Cu-Kα radiation for L^1. All data were corrected for Lorentz and polarization effects. Absorption corrections were also applied for L^1 (psi-scan) and $[ZnL^1](NO_3)_2\cdot 2H_2O$, $[Ag_2L^1(NO_3)_2]$ and $[Ag_2L^1](ClO_4)_2\cdot 4CH_3CN$ (empirical).[22] Complex scattering factors were taken from the program package SHELXTL.[23] The structures were solved by direct methods, which revealed the position of all non-hydrogen atoms. All the structures were refined on F^2 by a full-matrix least-squares procedure using anisotropic displacement parameters for all non-hydrogen atoms. The hydrogen atoms were located in their calculated positions and refined using a riding model.

CCDC reference numbers 185884–185887.

See http://www.rsc.org/suppdata/dt/b2/b204694f/ for crystallographic data in CIF or other electronic format.

Acknowledgements

We thank Xunta de Galicia (PGIDT01PXI20901PR) for financial support. Intensity measurements were performed at the Unidade de Raios X. RIAIDT, University of Santiago de Compostela, Spain.

References

1 A. Bianchi, M. Micheloni and P. Paoletti, *Coord. Chem. Rev.*, 1991, **110**, 17 and refs. therein.
2 E. C. Constable, M. G. B. Drew, G. Forsyth and M. D. Ward, *J. Chem. Soc., Chem. Commun.*, 1988, 1450.
3 D. E. Fenton, R. W. Matthews, M. McPartlin, B. P. Murphy, I. J. Scowen and P. A. tasker, *J. Chem. Soc., Chem. Commun.*, 1994, 1391.
4 L. H. Bryant, Jr., A. Lachgar, K. S. Coates and S. C. Jackels, *Inorg. Chem.*, 1994, **33**, 2219.
5 G. L. Rothermel, Jr., L. Miao, A. L. Hill and S. C. Jackels, *Inorg. Chem.*, 1992, **31**, 4854.
6 S. W. Annie Bligh, N. Choi, E. G. Evagoras, W. Li and M. McPartlin, *J. Chem. Soc., Chem. Commun.*, 1994, 2399.
7 L. Tei, V. Lippolis, A. J. Blake, P. A. Cooke and M. Schröder, *Chem. Commun.*, 1998, 2633; H. Aneetha, Y.-H. Lai, S.-C. Lin, K. Panneerselvam, T.-H. Lu and S.-C. Chung, *J. Chem. Soc., Dalton Trans.*, 1999, 2885.
8 R. Bandín, R. Bastida, A. de Blas, P. Castro, D. E. Fenton, A. Macías, A. Rodríguez and T. Rodríguez-Blas, *J. Chem. Soc., Dalton Trans.*, 1994, 1185; R. Bastida, A. de Blas, P. Castro, D. E. Fenton, A. Macías, R. Rial, A. Rodríguez and T. Rodríguez-Blas, *J. Chem. Soc., Dalton Trans.*, 1996, 1493; L. Valencia, R. Bastida, A. de Blas, D. E. Fenton, A. Macías, A. Rodríguez, T. Rodríguez-Blas and A. Castiñeiras, *Inorg. Chim. Acta*, 1998, **282**, 42; H. Adams, R. Bastida, D. E. Fenton, A. Macías, S. E. Spey and L. Valencia, *Inorg. Chem. Commun.*, 1999, **2**, 513; H. Adams, R. Bastida, D. E. Fenton, B. E. Mann and L. Valencia, *Eur. J. Org. Chem.*, 1999, 1843; L. Valencia, H. Adams, R. Bastida, A. de Blas, D. E. Fenton, A. Macías, A. Rodríguez and T. Rodríguez-Blas, *Inorg. Chim. Acta*, 2000, **300–302**, 234; L. Valencia, H. Adams, R. Bastida, D. E. Fenton and A. Macías, *Inorg. Chim. Acta*, 2001, **317**, 45; L. Valencia, H. Adams, R. Bastida, D. E. Fenton, A. Macías, J. Mahía and S. E. Spey, *Polyhedron*, 2001, **20**, 3091; H. Adams, R. Bastida, D. E. Fenton, A. Macías, S. E. Spey and L. Valencia, *J. Chem. Soc., Dalton Trans.*, 1999, 4131.
9 J. F. Carvalho, S. P. Crofts, S. M. Rocklage, *PCT Patent Application No. WO 91/10645 (EP 91/00126)*, July 25, 1991.
10 W. D. Kim, Chem. Dissertation, The University of Texas at Dallas, Richardson, TX, 1994.
11 K. Nakamoto, *Infrared and Raman Spectra of Inorganic and Coordination Compounds*, Wiley-Interscience, New York, 3rd edn., 1978.

12 W. J. Geary, *Coord. Chem. Rev.*, 1971, **7**, 181.
13 N. S. Gill, R. H. Nuttall, D. E. Scaife and D. W. Sharp, *J. Inorg. Nucl. Chem.*, 1961, **18**, 79.
14 M. F. Rosenthal, *J. Chem. Educ.*, 1973, **50**, 331; A. J. Hathaway and A. E. Underhill, *J. Chem. Soc.*, 1961, 3091.
15 A. J. Hathaway and A. E. Underhill., *J. Chem. Soc.*, 1961, 3091.
16 W. T. Carnall, S. Siegel, J. R. Ferraro, B. Tani and E. Gebert, *Inorg. Chem.*, 1973, **12**, 560.
17 P. Gueriero, U. Casellato, S. Tamburini, P. A. Vigato and R. Graziani, *Inorg. Chim. Acta*, 1987, **129**, 127.
18 L. H. Bryant, Jr., A. Lachgar and S. C. Jackels, *Inorg. Chem.*, 1995, **34**, 4230.
19 W. J. Eilbeck, F. Holmes and A. E. Underhill, *J. Chem. Soc. A*, 1967, 757.
20 A. B. P. Lever, *Inorganic Electronic Spectroscopy*, 2nd edn., Elsevier, Amsterdam, 1984.
21 B. N. Figgis, *Introduction to Ligand Fields*, Interscience, New York, 1967.
22 G. M. Sheldrick, Sadabs, Program for empirical absorption correction of area detector data, University of Göttingen, Germany, 1996.
23 SHELXTL version, An integrated system for solving and refining crystal structures from diffraction data (Revision 5.1), Bruker AXS Ltd., Madison, WI.